

Extra-articular, Intraepiphyseal Drilling for Osteochondritis Dissecans of the Knee

Characterization of a Safe and Reproducible Surgical Approach

Cody S. Lee,* BS, Christopher G. Larsen,[†] MD, Daniel A. Marchwiany,[‡] MD, and Steven C. Chudik,^{§||¶} MD

Investigation performed at Hinsdale Orthopaedics, Westmont, Illinois, USA

Background: Osteochondritis dissecans (OCD) is an idiopathic focal condition affecting the subchondral bone of joints, and it is increasingly prevalent among the active young adult population. For lesions that have failed nonoperative management, trans-articular drilling and extra-articular drilling are surgical options. Although the extra-articular approach preserves the articular cartilage, it is technically challenging and could benefit from a study of surgical approach.

Purpose: To use 3-dimensional modeling of magnetic resonance imaging (MRI) scans from skeletally immature individuals to characterize safe tunnel entry points, trajectories, and distances from the physeal and articular cartilage along the course of the distal femoral epiphysis to the OCD target in their most common location of the medial femoral condyle (MFC).

Study Design: Descriptive laboratory study.

Methods: A total of 17 MRI scans from skeletally immature patients were used to create 3-dimensional models of the knee joint. Virtual representations of an OCD lesion were placed in the lateral aspect of the MFC; cylinders simulating tunnel length, diameter, and trajectory were superimposed onto the models; and measurements were taken.

Results: Two safe tunnels were identified, 1 anterior and 1 posterior to the medial collateral ligament (MCL). The anterior tunnel had a diameter of 10.3 ± 1.4 mm, skin entry point of 16.9 ± 12.1 mm anterior and 7.1 ± 5.9 mm superior to the medial epicondyle, bony entry point of 12.1 ± 3.5 mm anterior and 2.4 ± 3.5 mm inferior to the medial epicondyle, and tunnel length of 31.8 ± 3.7 mm. The posterior tunnel had a diameter of 7.8 ± 1.8 mm, skin entry point of 9.4 ± 5.1 mm posterior and 26.0 ± 14.0 mm superior to the medial epicondyle, bony entry point of 8.6 ± 2.6 mm posterior and 5.1 ± 4.2 mm superior to the medial epicondyle, and tunnel length of 33.5 ± 4.5 mm.

Conclusion: This anatomic characterization study identifies and defines 2 safe and reproducible tunnel approaches, 1 anterior and 1 posterior to the MCL, for drilling or creating tunnels to OCD lesions of the MFC in an extra-articular fashion.

Clinical Relevance: The study findings provide valuable anatomic references for surgeons performing extra-articular drilling or tunneling of OCD lesions.

Keywords: anatomy; imaging; tunnel; juvenile

Osteochondritis dissecans (OCD) is an idiopathic focal condition affecting the subchondral bone of joints and is increasingly prevalent among the active young adult population, likely due to increased participation in athletics.¹⁹ Although the cause of this condition is unknown, leading theories suggest that repetitive microtrauma, ischemia, genetic influences, and growth disturbances may play a role in the pathophysiological process.²⁹ A recent

retrospective study determined that the incidence of OCD among children ages 6 to 19 years is 15.4 and 3.3 per 100,000 for males and females, respectively, with 3.3 times more cases in 12- to 19-year-olds compared with 6- to 11-year-olds.¹⁷ Lesions most commonly affect the knee joint and are predominantly (70%-80%) located in the lateral aspect of the medial femoral condyle (MFC).^{7,10,11,23} Early diagnosis is important, as lesion stability and skeletal maturity influence treatment options and clinical outcomes. Stable OCD lesions are defined as those with intact overlying articular cartilage and that generally represent an early stage of the disease when identified in skeletally

The Orthopaedic Journal of Sports Medicine, 7(2), 2325967119830397

DOI: 10.1177/2325967119830397

© The Author(s) 2019

This open-access article is published and distributed under the Creative Commons Attribution - NonCommercial - No Derivatives License (<http://creativecommons.org/licenses/by-nc-nd/4.0/>), which permits the noncommercial use, distribution, and reproduction of the article in any medium, provided the original author and source are credited. You may not alter, transform, or build upon this article without the permission of the Author(s). For article reuse guidelines, please visit SAGE's website at <http://www.sagepub.com/journals-permissions>.

immature individuals (juvenile OCD). Most cases of stable juvenile OCD will heal without surgery, so numerous authors agree that nonoperative management is the preferred initial treatment modality in the skeletally immature population with stable OCD lesions.^{5,7,10-12,19,23,28,29} Therefore, failure of nonoperative management for stable lesions is a general indication for surgical intervention.²⁹

Arthroscopic drilling of OCD lesions with a K-wire is well established in the literature as a surgical treatment option for stable OCD lesions smaller than 2.5 cm² that have failed nonoperative treatment. This technique creates vascular channels from the underlying bone marrow to stimulate revascularization and healing of the damaged subchondral bone.^{4,10,12,19} Multiple case series have described good radiographic and clinical outcomes for both transarticular and extra-articular approaches for arthroscopic drilling.^{1,12} Transarticular or transchondral drilling is performed by penetrating the overlying articular cartilage under direct arthroscopic visualization of the OCD lesion, whereas extra-articular or retroarticular drilling occurs through the affected femoral condyle, sparing the articular cartilage.²⁹ Transarticular drilling is technically more facile; however, the potential long-term consequences associated with violating the intact articular cartilage are concerning. In contrast, extra-articular drilling preserves the articular cartilage; however, it is technically more challenging, requires fluoroscopic guidance, and increases the risk of insufficient drilling depth and injury to surrounding soft tissues and the physis.^{2,12,16} A recent survey of members of the Pediatric Orthopaedic Society of North America revealed that for treatment of stable OCD lesions that have failed nonoperative management, 53.5% of respondents prefer extra-articular drilling whereas 32.6% prefer transarticular drilling, indicating a trend toward the technique that leaves articular cartilage intact.³⁰

The purpose of this study was to use 3-dimensional modeling of magnetic resonance imaging (MRI) scans from skeletally immature individuals to characterize safe tunnel entry points, trajectories, and distances from the physeal and articular cartilage along the course of the distal femoral epiphysis to the OCD target in their most common location of the MFC. Our objective was to define reproducible safe portals and landmarks for extra-articular drilling that will allow for more surgeons to become comfortable performing this technique, thereby reducing the amount of intraoperative fluoroscopy and radiation exposure while decreasing the risk of injury to surrounding structures and cartilage. We hypothesized that analysis of 3-dimensional modeling of MRIs of skeletally immature patients would

allow us to define reproducible surgical tunnel approaches for treatment of OCD lesions of the MFC both anterior and posterior to the medial collateral ligament.

METHODS

With an institutional review board–approved protocol, MRI studies were obtained from 17 skeletally immature patients with open distal femoral physes and normal knee structure. Of the 17 patients, 10 were male and 7 were female, with a mean age of 12.7 years (range, 9–15 years). MRI of the knee was performed by use of a 1.5-T scanner with 3 mm to 4 mm–thick, 2-dimensional proton density and T1-weighted imaging sequences in the axial, coronal, and sagittal planes. DICOM images from the MRI data sets were imported into Mimics (version 16.0; Materialise) and 3-matic (version 8.0; Materialise) computer software to create a 3-dimensional model of the knee, to simulate surgical approaches, and to measure relevant anatomic relationships.

The bone, physis, articular cartilage, and relevant soft tissue structures were manually mapped in the sagittal image set to create masks used to generate 3-dimensional models of the knee. The manual mapping was done by a single member of the research team who was trained in this process (D.A.M.). After multiple trials were performed to refine the technique, the final mapping was completed; reported values are the average of multiple measurements. The medial epicondyle was identified and defined by a single point corresponding to its most prominent aspect. The borders of the medial collateral ligament (MCL) were outlined in the axial and coronal image sets in order to identify and define the entire footprint of the MCL femoral origin. Mimics software was used to overlay these structures onto the 3-dimensional models.

Virtual representations of stable OCD lesions were designed and placed in the classic location, the lateral aspect of the MFC, to serve as the target for simulated tunnels. This was done by creating a hemispheric-shaped lesion using the computer software to select for the intersection of bone and a computer-generated sphere formed to the contours of the femoral condyle and placed in the classic OCD location. The average lesion length (measured in the sagittal view), width (measured in coronal view), and surface area of the simulated lesions were 16.6 ± 0.54 mm, 14.9 ± 0.68 mm, and 248.9 ± 16.5 mm², respectively. These parameters were consistent with the reported values of Wall et al,²⁸ who examined the healing potential of stable juvenile OCD lesions.

§Address correspondence to Steven C. Chudik, MD, Hinsdale Orthopaedics, 1010 Executive Court #250, Westmont, IL 60559, USA (email: steven@chudikmd.com) (Twitter: @StevenChudik).

*University of Chicago, Pritzker School of Medicine, Chicago, Illinois, USA.

†Department of Orthopaedic Surgery, Zucker School of Medicine at Hofstra/Northwell, New Hyde Park, New York, USA.

‡Department of Orthopaedic Surgery, University of North Carolina, Chapel Hill, North Carolina, USA.

||Hinsdale Orthopaedics, Westmont, Illinois, USA.

¶Orthopaedic Surgery and Sports Medicine Teaching and Research Foundation, Westmont, Illinois, USA.

One or more of the authors has declared the following potential conflict of interest or source of funding: S.C.C. is a paid consultant for Arthrex, receives royalties from Arthrex, and receives educational support from Medwest Associates. AOSSM checks author disclosures against the Open Payments Database (OPD). AOSSM has not conducted an independent investigation on the OPD and disclaims any liability or responsibility relating thereto.

Ethical approval for this study was obtained from the Loyola University Institutional Review Board.

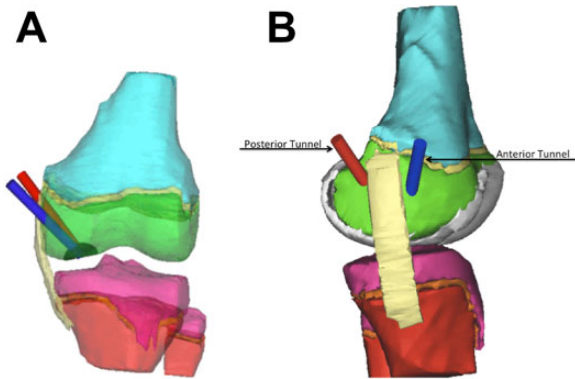


Figure 1. (A) Coronal view of the anterior (blue) and posterior (red) tunnel approaches. Tunnels traverse the epiphysis (green) and end at the center of the simulated osteochondritis dissecans lesion (dark hemisphere). (B) Sagittal view of the anterior and posterior tunnel approaches.

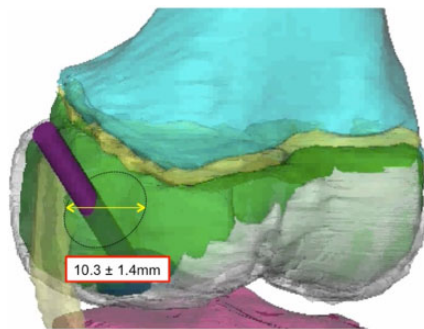


Figure 2. Tunnel diameter for the “window of safety” for the anterior approach.

To simulate extra-articular tunnels, cylinders were superimposed into the 3-dimensional models. A cylinder was placed starting from either an anterior or a posterior entry point relative to the MCL origin, traversing the epiphysis and ending at the center of the lesion (Figure 1). To determine anterior and posterior “windows of safety,” we measured the largest tunnel diameter capable of safely traversing the epiphysis without contacting the borders of the MCL and remaining no less than 10 mm from the femoral physis and articular cartilage (Figure 2). The value of 10 mm was chosen as a minimum safe distance to minimize the risk of drilling-associated thermal osteonecrosis. The temperature generated during drilling is multifactorial and depends on the drill diameter, drill speed, use of cooling, drilling depth, drilling duration, and bone thickness, along with various other drill specifications and drilling parameters.^{3,22} We chose the 10-mm distance from the edge of our tunnel, as this was the reported width of maximum temperature distribution in 1 study³ that evaluated the spatial distribution of temperature while drilling.

We measured the distance from the center of the tunnel to the medial epicondyle, the length of the tunnel to the OCD lesion, and the angle made by a line through the

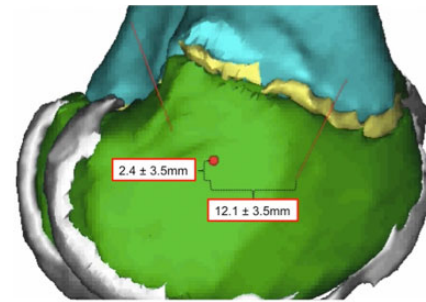


Figure 3. Bony entry point for the anterior approach relative to the medial collateral ligament insertion point (red dot).

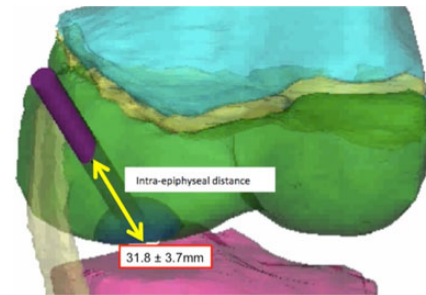


Figure 4. Tunnel length of the anterior approach, measured from the bony entry point to the center of the lesion.

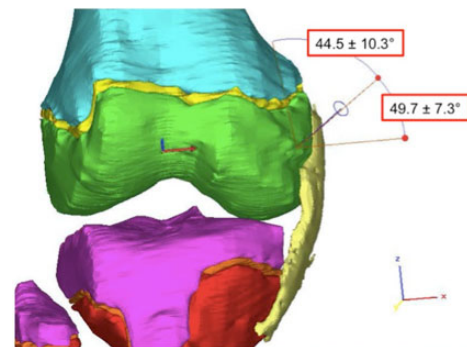


Figure 5. Tunnel trajectory in the coronal plane for the anterior approach with angle references to both the longitudinal axis of the femur and the joint line.

center of the tunnel relative to the longitudinal axis of the femur and to the femoral joint line in both the coronal and the sagittal planes (Figures 3-6). Additionally, because this procedure is often performed with the knee in a flexed position,^{9,24} we simulated knee flexion and rotated the MCL around a fulcrum defined by its insertion point in 15° increments up to a maximum of 90° to determine how the degree of knee flexion affected the size of the window (Figure 7).

Mimics and 3-Matic software tools were used to collect all singular data points. Statistical analysis was performed with Microsoft Excel (version 2011). Continuous variables are reported with means and standard deviations.

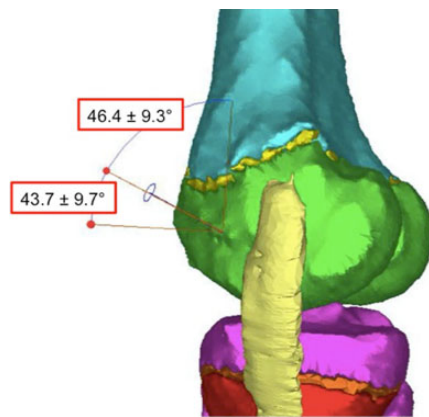


Figure 6. Tunnel trajectory in the sagittal plane for the anterior approach with angle references to both the longitudinal axis of the femur and the joint line.

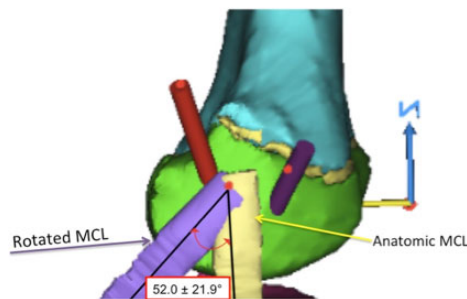


Figure 7. Knee flexion was simulated by rotating the medial collateral ligament (MCL) on its point of insertion. Measurements were taken at 15° increments to determine how the degree of knee flexion affected the size of the window.

RESULTS

Anterior Window, Tunnel Anterior to the MCL Origin

The anterior “safe window” allowed a maximal tunnel diameter of 10.3 ± 1.4 mm (Table 1). The tunnel entered the skin at a point 16.9 ± 12.1 mm anterior and 7.1 ± 5.9 mm superior to the medial epicondyle and penetrated the bone 12.1 ± 3.5 mm anterior and 2.4 ± 3.5 mm inferior to the medial epicondyle. The average epiphyseal tunnel length was 31.8 ± 3.7 mm. In the coronal plane, the angle of the tunnel relative to the longitudinal axis of the femur was $44.5^\circ \pm 10.3^\circ$; to the femoral joint line it was $49.7^\circ \pm 7.3^\circ$. In the sagittal plane, the angle of the tunnel relative to the longitudinal axis of the femur was $46.4^\circ \pm 9.3^\circ$; to the femoral joint line it was $43.7^\circ \pm 9.7^\circ$. The anterior safe window was not affected by knee flexion.

Posterior Window, Tunnel Posterior to the MCL Origin

The posterior “safe window” allowed a maximal tunnel diameter of 7.8 ± 1.8 mm (Table 2). The tunnel entered the skin 9.4 ± 5.1 mm posterior and 26.0 ± 14.0 mm superior to the

TABLE 1
Values for the Anterior Window of Safety
Obtained From 3-Dimensional Imaging Analysis^a

Tunnel length, mm	31.8 ± 3.7	
Tunnel diameter, mm	10.3 ± 1.4	
	Anterior to Medial Epicondyle	Superior/Inferior to Medial Epicondyle
Skin entry point, mm	16.9 ± 12.1	7.1 ± 5.9 superior
Bone entry point, mm	12.1 ± 3.5	2.4 ± 3.5 inferior
	In Reference to Joint Line	In Reference to Longitudinal Axis of Femur
Coronal angle, deg	49.7 ± 7.3	44.5 ± 10.3
Sagittal angle, deg	43.7 ± 9.7	46.4 ± 9.3

^aData are reported as mean \pm SD.

TABLE 2
Values for the Posterior Window of Safety
Obtained From 3-Dimensional Imaging Analysis^a

Tunnel length, mm	33.5 ± 4.5	
Tunnel diameter, mm	7.8 ± 1.8	
	Posterior to Medial Epicondyle	Superior to Medial Epicondyle
Skin entry point, mm	9.4 ± 5.1	26.0 ± 14.0
Bone entry point, mm	8.6 ± 2.6	5.1 ± 4.2
	In Reference to Joint Line	In Reference to Longitudinal Axis of Femur
Coronal angle, deg	50.7 ± 9.3	43.9 ± 10.0
Sagittal angle, deg	81.8 ± 8.8	10.8 ± 6.9

^aData are reported as mean \pm SD.

medial epicondyle and penetrated the bone 8.6 ± 2.6 mm posterior and 5.1 ± 4.2 mm superior to the medial epicondyle. The average epiphyseal tunnel length was 33.5 ± 4.5 mm. In the coronal plane, the angle of the tunnel relative to the longitudinal axis of the femur was $50.7^\circ \pm 9.3^\circ$; to the femoral joint line it was $50.7^\circ \pm 9.3^\circ$. In the sagittal plane, the angle of the tunnel relative to the longitudinal axis of the femur was $10.8^\circ \pm 6.9^\circ$; to the femoral joint line it was $81.8^\circ \pm 8.8^\circ$. The MCL began to narrow the posterior window as the knee flexion angle reached $52.0^\circ \pm 21.9^\circ$.

DISCUSSION

When indicated, arthroscopic drilling for stable juvenile OCD lesions, in both transarticular^{13,18,20} and extra-articular fashion,^{2,4,8,9,16,21} has been shown to be an effective treatment modality with minimal complications. The extra-articular approach maintains the theoretical benefit of avoiding injury to the intact articular cartilage but is

more technically challenging, requiring intraoperative fluoroscopy and significant radiation exposure.^{2,4,7-11,16} Inadequate drilling of OCD lesions and accidental soft tissue injuries to the skin and ligaments of the knee are not uncommon.⁶ Despite the increased technical difficulty, results in the literature regarding extra-articular drilling have been encouraging. Edmonds et al⁹ reported that in a retrospective study of 59 patients treated with extra-articular drilling, 75% of juvenile OCD lesions demonstrated radiographic healing 12 months after treatment and 98% at 36 months. In a case series of 12 patients treated with extra-articular drilling, Donaldson and Wojtys⁸ reported excellent outcomes for all 12 of their study patients, with radiographic healing on average at 8.5 months. In a case series involving 31 patients, Boughanem et al⁴ reported significant improvements in outcome scores and radiographic evidence of healing in all cases.

Although intraoperative fluoroscopy is usually used for guidance during the technique of extra-articular drilling, other methods have been described in the literature. Mechanical targeting devices (eg, drill guides) have been developed, but their utility is limited due to the bulkiness of their design and the tightly ligamentous, constrained knee joints seen in young athletes.¹⁴ Electromagnetic guidance systems and MRI guidance have been described for use with extra-articular drilling of OCD lesions, but their applications are still largely experimental.^{14,15,25}

Our study affirmed our hypothesis and described reproducible safe windows for extra-articular drilling of OCD lesions of the MFC. We discovered 2 safe windows, 1 anterior and 1 posterior to the MCL, and described associated superficial bony landmarks on the MFC, the angle of trajectory, and the tunnel length associated with an extra-articular epiphyseal approach to OCD lesions of the MFC to assist surgeons. Additionally, the study has helped describe potential for drilling tunnels of sufficient diameter to allow extra-articular drilling, debridement, and bone grafting.

Limitations of our study include using MRIs with a slice thickness of up to 3.5 mm in the sagittal plane, which restricts the resolution and accuracy of our 3-dimensional models. To limit this effect, we used all 3 MRI cross sections (axial, coronal, and sagittal) to better identify and position the relevant landmarks despite losing some data between slices. Recent studies by Swami et al^{26,27} showed good reliability when using 2-dimensional MRIs to localize knee anatomic features for ACL reconstruction, and those investigators concluded that there is no significant difference in accuracy with this technique compared with using higher resolution, 3-dimensional MRI sequences. Additionally, the safe portals described in our study apply to OCD lesions of the lateral aspect of the MFC only. Although this is the most common location for juvenile OCD lesions, lesions are sometimes seen in the lateral femoral condyle and even more rarely in the patella and trochlea. Defect size varies between patients, and this study is limited by its assumptions made by simulating standard lesions. However, the models in this study yielded a generous average defect size of 248.9 mm², and the tunnel parameters defined in this study are safe and inclusive for drilling the majority of

lesion sizes recommended for treatment. A further limitation is the inherent anatomic variability that exists between patients. Patient body mass index at the time of MRI, which presumably affects the patient's soft tissue envelope, was unavailable. Differences in soft tissue envelope between patients will affect skin entry points, and it is still recommended to use radiographic guidance to confirm positioning for drilling during surgery.

CONCLUSION

This anatomic characterization study identifies and defines 2 safe and reproducible tunnel approaches, 1 anterior and 1 posterior to the MCL, for drilling or creating tunnels to OCD lesions of the MFC in an extra-articular fashion. From our study, the characterization of anterior and posterior drilling tunnels for the treatment of juvenile OCD lesions of the MFC can guide surgeons during surgery and theoretically help minimize the use of intraoperative fluoroscopy and reduce the risk of iatrogenic injury to surrounding structures including the articular and physeal cartilage.

REFERENCES

1. Abouassaly M, Peterson D, Salci L, et al. Surgical management of osteochondritis dissecans of the knee in the paediatric population: a systematic review addressing surgical techniques. *Knee Surg Sports Traumatol Arthrosc.* 2014;22(6):1216-1224.
2. Adachi N, Deie M, Nakamae A, Ishikawa M, Motoyama M, Ochi M. Functional and radiographic outcome of stable juvenile osteochondritis dissecans of the knee treated with retroarticular drilling without bone grafting. *Arthroscopy.* 2009;25(2):145-152.
3. Augustin G, Davila S, Udiljak T, Vedrina DS, Bagatin D. Determination of spatial distribution of increase in bone temperature during drilling by infrared thermography: preliminary report. *Arch Orthop Trauma Surg.* 2009;129(5):703-709.
4. Boughanem J, Riaz R, Patel RM, Sarwark JF. Functional and radiographic outcomes of juvenile osteochondritis dissecans of the knee treated with extra-articular retrograde drilling. *Am J Sports Med.* 2011;39(10):2212-2217.
5. Cahill BR. Osteochondritis dissecans of the knee: treatment of juvenile and adult forms. *J Am Acad Orthop Surg.* 1995;3(4):237-247.
6. Citak M, Kendoff D, Stubig T, et al. Drilling with 3D fluoroscopic navigation in osteonecrosis of the femoral condyle. *Unfallchirurg.* 2008;111(5):344-349.
7. Dettlerline AJ, Goldstein JL, Rue JP, Bach BR Jr. Evaluation and treatment of osteochondritis dissecans lesions of the knee. *J Knee Surg.* 2008;21(2):106-115.
8. Donaldson LD, Wojtys EM. Extraarticular drilling for stable osteochondritis dissecans in the skeletally immature knee. *J Pediatr Orthop.* 2008;28(8):831-835.
9. Edmonds EW, Albright J, Bastrom T, Chambers HG. Outcomes of extra-articular, intra-epiphyseal drilling for osteochondritis dissecans of the knee. *J Pediatr Orthop.* 2010;30(8):870-878.
10. Edmonds EW, Polousky J. A review of knowledge in osteochondritis dissecans: 123 years of minimal evolution from König to the ROCK study group. *Clin Orthop Relat Res.* 2013;471(4):1118-1126.
11. Erickson BJ, Chalmers PN, Yanke AB, Cole BJ. Surgical management of osteochondritis dissecans of the knee. *Curr Rev Musculoskelet Med.* 2013;6(2):102-114.
12. Gunton MJ, Carey JL, Shaw CR, Murnaghan ML. Drilling juvenile osteochondritis dissecans: retro- or transarticular? *Clin Orthop Relat Res.* 2013;471(4):1144-1151.

13. Hayan R, Phillippe G, Ludovic S, Claude K, Jean-Michel C. Juvenile osteochondritis of femoral condyles: treatment with transchondral drilling. Analysis of 40 cases. *J Child Orthop*. 2010;4(1):39-44.
14. Hoffmann M, Peterson JP, Schroder M, et al. Accuracy analysis of a novel electromagnetic navigation procedure versus a standard fluoroscopic method for retrograde drilling of osteochondritis dissecans lesions of the knee. *Am J Sports Med*. 2012;40(4):920-926.
15. Hoffman M, Schroder M, Reuger JM. A novel computer navigation system for retrograde drilling of osteochondral lesions. *Sports Med Arthrosc Rev*. 2014;22(4):215-218.
16. Kawasaki K, Uchio Y, Adachi N, Iwasa J, Ochi M. Drilling from the intercondylar area for treatment of osteochondritis dissecans of the knee joint. *Knee*. 2003;10(3):257-263.
17. Kessler JL, Nikizad H, Shea KG, et al. The demographics and epidemiology of osteochondritis dissecans of the knee in children and adolescents. *Am J Sports Med*. 2014;42(2):320-326.
18. Kocher MS, Micheli LJ, Yaniv M, Zurakowski D, Ames A, Adrignolo AA. Functional and radiographic outcome of juvenile osteochondritis dissecans of the knee treated with transarticular arthroscopic drilling. *Am J Sports Med*. 2001;29(5):562-566.
19. Kocher MS, Tucker R, Ganley TJ, Flynn JM. Management of osteochondritis dissecans of the knee: current concepts review. *Am J Sports Med*. 2006;34(7):1181-1191.
20. Louisia S, Beaufils P, Katabi M, Robert H; French Society of Arthroscopy. Transchondral drilling for osteochondritis dissecans of the medial condyle of the knee. *Knee Surg Sports Traumatol Arthrosc*. 2003;11(1):33-39.
21. Ojala R, Kerimaa P, Lakovaara M, et al. MRI-guided percutaneous retrograde drilling of osteochondritis dissecans of the knee. *Skeletal Radiol*. 2011;40(6):765-770.
22. Pandey RK, Panda SS. Drilling of bone: a comprehensive review. *J Clin Orthop Trauma*. 2013;4(1):15-30.
23. Pascual-Garrido C, McNickle AG, Cole BJ. Surgical treatment options for osteochondritis dissecans of the knee. *Sports Health*. 2009;1(4):326-334.
24. Pennock AT, Bomar JD, Chambers HG. Extra-articular, intraepiphyseal drilling for osteochondritis dissecans of the knee. *Arthrosc Tech*. 2013;2(3):e231-e235.
25. Seebauer CJ, Bail HJ, Rump JC, et al. Advancements in orthopedic intervention: retrograde drilling and bone grafting of osteochondral lesions of the knee using magnetic resonance imaging guidance. *Cardiovasc Intervent Radiol*. 2010;33(6):1230-1234.
26. Swami VG, Cheng-Baron J, Hui C, Thompson R, Jaremko JL. Reliability of estimates of ACL attachment locations in 3-dimensional knee reconstruction based on routine clinical MRI in pediatric patients. *Am J Sports Med*. 2013;41(6):1319-1329.
27. Swami VG, Mabee M, Hui C, Jaremko JL. MRI anatomy of the tibial ACL attachment and proximal epiphysis in a large population of skeletally immature knees: reference parameters for planning anatomic physeal-sparing ACL reconstruction. *Am J Sports Med*. 2014;42(7):1644-1651.
28. Wall EJ, Vourazeris J, Myer GD, et al. The healing potential of stable juvenile osteochondritis dissecans knee lesions. *J Bone Joint Surg Am*. 2008;90(12):2655-2664.
29. Winthrop Z, Pinkowsky G, Hennrikus W. Surgical treatment for osteochondritis dissecans of the knee. *Curr Rev Musculoskelet Med*. 2015;8(4):467-475.
30. Yellin JL, Gans I, Carey JL, et al. The surgical management of osteochondritis dissecans of the knee in the skeletally immature: a survey of the Pediatric Orthopaedic Society of North America (POSNA) membership. *J Pediatr Orthop*. 2017;37(7):491-499.